Eur. Phys. J. D **37**, 313–317 (2006)
DOI: 10.1140/epjd/e2005-00313-4

THE EUROPEAN PHYSICAL JOURNAL D

Precise measurement of hyperfine structure in the $5^2P_{1/2}$ state of Rb

D. Das and V. Natarajan[a]

Department of Physics, Indian Institute of Science, Bangalore 560 012, India

Received 2nd August 2005 / Received in final form 14 October 2005
Published online 22 November 2005 –

Abstract. We have measured hyperfine structure in the $5^2P_{1/2}$ state of Rb using a frequency-stabilized diode laser, which is locked to one hyperfine transition, and an acousto-optic modulator, whose frequency is locked to the interval of interest. We check for optical-pumping errors by repeating the measurement at different values of pump power in the saturated-absorption spectrometer. We obtain precise values of the hyperfine constant: $A = 120.645(5)$ MHz for ^{85}Rb and $A = 406.119(7)$ MHz for ^{87}Rb. The values resolve a large discrepancy between two earlier high-accuracy measurements on this state.

PACS. 32.10.Fn Fine and hyperfine structure – 42.62.Fi Laser spectroscopy – 42.55.Px Semiconductor lasers; laser diodes

1 Introduction

Precise measurement of hyperfine structure in atoms provides valuable information about the atomic wavefunction in the vicinity of the nucleus [1,2]. The exact knowledge of atomic wavefunctions is particularly important in heavy alkali atoms because of their use in experiments such as atomic signatures of parity violation [3,4] and search for a permanent electric-dipole moment [5]. In earlier work [6], we have developed a technique to measure hyperfine intervals in excited states with high accuracy. The technique combines the advantage of the narrow linewidth offered by tunable diode lasers with the fact that an acousto-optic modulator (AOM) provides calibrated frequency shifts. The rf frequency driving the AOM is directly locked to the hyperfine interval of interest. We had earlier applied this technique to the $5^2P_{3/2}$ state of Rb and demonstrated a precision of 20 kHz.

In this work, we measure intervals in the $5^2P_{1/2}$ state of Rb (D_1 line) with 7 kHz precision. The increased accuracy is made possible by two improvements in our technique: double-passing through the AOM to maintain directional stability, and use of a magnetic shield around the cell to reduce Zeeman broadening of the linewidth. The measurement on the $5^2P_{1/2}$ state of Rb is motivated by an important consideration: there are two recent high-accuracy measurements of the hyperfine constant in ^{87}Rb, with a value of 408.328(15) MHz in reference [7] and a value of 406.147(15) MHz from our laboratory [8]. The two values claim 15 kHz accuracy, but differ by nearly 100σ (combined). The first value is also somewhat discrepant with the recommended value of 406.2(8) MHz [1]. There is a smaller discrepancy of 6.3σ in the value for ^{85}Rb. Our current work agrees well with our earlier results, even though the methods used for the two measurements are different.

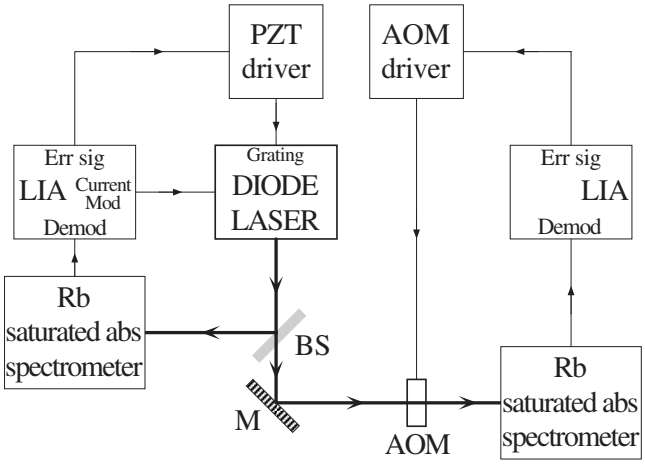

Fig. 1. Schematic of the experiment. Figure key – PZT: piezoelectric transducer, AOM: acousto-optic modulator, LIA: lock-in amplifier, BS: beam splitter, M: mirror.

2 Experimental details

The experimental schematic is shown in Figure 1 and is essentially the same as described in our earlier work [6]. The output from a grating-stabilized diode laser is split

[a] e-mail: vasant@physics.iisc.ernet.in

into two parts. The first part goes into a Rb saturated-absorption spectrometer, the error signal from which is used to lock the laser to a particular hyperfine transition. The second part passes through an AOM and then goes into another Rb saturated-absorption spectrometer. The error signal from a neighboring hyperfine transition is fed back to lock the AOM at the difference frequency. Thus the AOM frequency directly gives the interval we are measuring. For measuring larger intervals not accessible with a single AOM, we use an additional AOM with a fixed frequency offset (not shown). To ensure that the pump and probe beams in the saturated-absorption spectrometer are perfectly counter-propagating, we use orthogonal linear polarizations for the beams and use polarizing beam-splitter cubes to mix and separate them. This configuration also allows precise control over the individual beam powers by using half-wave retardation plates in front of the cubes.

As mentioned earlier, we have made a couple of key improvements to the set up from our earlier work. First, we double pass through the AOM in order to maintain directional stability of the beam when the AOM frequency changes. Otherwise, changes in the direction of the beam can cause unwanted broadening of the line and reduce the beam overlap. Second, we use special magnetic shields [9] around the cells to reduce linewidth broadening due to splitting of the Zeeman sublevels.

The rms linewidth of the diode laser (before locking) is about 300 kHz. The injection current is modulated at $f = 20$ kHz and the signal from the spectrometers is demodulated at $3f$ to obtain the error signals. Such third-harmonic detection provides narrow dispersive signals that are insensitive to the underlying Doppler profile or peak pulling from nearby transitions [10]. This ensures that we are locked to within a few kHz of line center. The spectroscopy is done in room-temperature vapor cells with density of $\sim 10^9$ atoms/cc.

The power into the two spectrometers is adjusted to obtain the best lineshape and the narrowest linewidth. Under these conditions, the power in the probe beam is typically 10 μW corresponding to an intensity of about 0.25 mW/cm^2, and the pump-beam power is 30 μW or an intensity of 0.75 mW/cm^2. A representative saturated-absorption spectrum as the laser is scanned across the $F = 1 \rightarrow F' = 2$ transition in ^{87}Rb is shown in Figure 2. The solid line is a Lorentzian fit showing that the peak is very symmetric near the center. The slight distortion near the ends is because the underlying Doppler profile has not been subtracted, but this is not a problem with third-harmonic error signals. As discussed in the next section, the pump power is varied over a large range to check for errors due to optical-pumping effects.

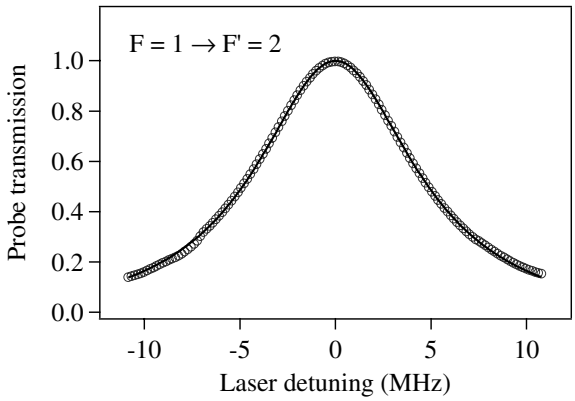

Fig. 2. Saturated-absorption spectrum in the Rb D_1 line. The open circles represent the measured probe-transmission signal (normalized) when the laser is tuned around the $F = 1 \rightarrow F' = 2$ transition in ^{87}Rb. The solid line is a Lorentzian fit. The slight distortion near the ends is due to the underlying Doppler profile, which is not subtracted.

3 Error analysis

3.1 Statistical errors

The primary sources of statistical error in our technique are the fluctuations in the lock point of the laser and the AOM. To minimize such effects, we use an integration time of 10 s in the frequency counter during each measurement of the AOM frequency. Then we take an average of 35−40 measurements for a given transition. This results in an overall statistical error of less than 2 kHz in each value. The timebase in the frequency counter used for measuring the AOM frequency has a stability of better than 10^{-6}, which translates to a negligible error of 100 Hz in the frequency measurement.

3.2 Systematic errors

Systematic errors can occur if there are systematic shifts in the lock-points of the laser and the AOM. This can arise due to several reasons.

(i) Shift in the peak position can occur due to (a) optical-pumping effects and (b) velocity redistribution of the atoms in the vapor cell due to radiation pressure [11]. Such effects manifest themselves as inversion of hyperfine peaks or distortion of the Lorentzian lineshape. As seen from Figure 2, the lineshape is quite symmetric. In addition, the beam intensities are much smaller than the saturation intensity of 1.64 mW/cm^2.

(ii) Line shifts from stray magnetic fields in the vicinity of the cells. The primary effect of a magnetic field is to split the Zeeman sublevels and broaden the line without affecting the line center. However, line shifts can occur if there is optical pumping into Zeeman sublevels. For a transition $(F, m_F) \rightarrow (F', m_{F'})$, the systematic shift of the line center is $\mu_B(g_{F'}m_{F'} - g_F m_F)B$, where $\mu_B = 1.4$ MHz/G is the Bohr magneton, g's denote the Landé g factors of the two levels, and B is the magnetic field. The selection rule for dipole transitions is $\Delta m = 0, \pm 1$, depending on the direction of the magnetic field (quantization axis) and the polarization of the light. Thus, if the beams are

perfectly linearly polarized, there will be no asymmetric driving and the line center is not affected. This is an important advantage of using polarizing beam-splitter cubes in the spectrometers; the extinction ratio of better than 1000:1 ensures near-perfect linear polarization of the beams. We further minimize these effects by using a magnetic shield around the cells. The residual field inside is measured with a 3-axis fluxgate magnetometer to be below 5 mG.

(iii) Shift in the lock point due to peak-pulling from neighboring transitions, the underlying Doppler profile, or phase shifts in the feedback loop. We minimize the first two effects by using third-harmonic detection for the error signals. We verify that the lineshape of the error signals is symmetric [8]. We check for phase-shift errors by using two AOMs with opposite frequency shifts. The first AOM is placed in the path of the first spectrometer, and produces a known frequency offset when the laser is locked to a given hyperfine peak. The second AOM (placed as usual in the path of the second spectrometer) is now locked to the *same* hyperfine peak. In other words, the same peak is used to lock both the laser and the AOM. Under these conditions, the second AOM should lock to the frequency of the first AOM, with any error arising solely due to phase-shift errors. We find that the second AOM tracks the frequency of the first AOM to within 1 kHz, showing that phase-shift errors cancel to a large degree because it is a difference measurement.

(iv) Shifts due to collisions in the vapor cells. Note that, theoretically, collisional shifts will be the same for different hyperfine components [12], and should cancel in a difference-frequency measurement. At the pressure inside the cell (0.2 mtorr), collisional shifts for each transition are estimated to be below 5 kHz. We further check for this error by repeating the experiment with vapor cells from different manufacturers, which have different background gases. We find that the measured values remain the same to within a few kHz.

One experimental parameter related to some of the above effects is the linewidth obtained in the saturated-absorption spectrum. As seen from Figure 2, the observed linewidth is about 10 MHz compared to the natural linewidth of 6 MHz. The primary cause for this increase is misalignment angle between the pump and probe beams, and power broadening from the pump beam. To confirm this, we have studied the variation of the linewidth as a function of pump power [13]. The linewidth extrapolated to zero power is only 6.5 MHz. This again shows that collisional broadening in the vapor cell is negligible. Without the magnetic shield, the linewidth increases by about 15%.

As mentioned in point (ii) above, the line center can be shifted in the presence of a residual magnetic field if there is *asymmetric* pumping into the Zeeman sublevels. Though this is not significant for linearly-polarized light, we have to consider that there will be a small ellipticity to the polarization. Thus, an important source of systematic error is line shifts due to optical-pumping effects in the presence of residual magnetic fields and residual ellipticity of the polarization. However, we have an experimental handle to check for this error, namely the pump-beam power. Optical pumping will generally increase with increase in pump power. Hence by repeating the measurement at different values of pump power, we can determine the size of this effect and extrapolate to zero power, if necessary.

Table 1. Error budget.

Source of error	Shift (kHz)	
	^{85}Rb	^{87}Rb
1. Optical pumping into Zeeman sublevels	3.1	3.5
2. Laser lock to peak center	2	2
3. AOM lock to peak center	2	2
4. Collisional shifts	5	5

The estimated size of the various sources of systematic error in the measured intervals are listed in Table 1. The size of the shift due to optical pumping into Zeeman sublevels is calculated by taking the maximum Zeeman shift in a residual field of 5 mG. Note that the shifts due to items (i), (iii), and (iv) above will be roughly the same for both transitions, and will cancel in a difference-frequency measurement. Other errors due to the second-order Doppler effect or wavefront curvature will also cancel in a difference measurement.

4 Results and discussion

The $5^2P_{1/2}$ state of Rb has only one hyperfine interval, which is ∼362 MHz in ^{85}Rb and ∼812 MHz in ^{87}Rb. However, the saturated-absorption spectrum has three peaks corresponding to the two hyperfine levels and one crossover resonance in between. In addition, there are two sets of transitions starting from the two ground hyperfine levels. Thus, it is possible to measure the same interval in several ways, depending on which transition is used for locking the laser and which transition for locking the AOM, and whether we upshift or downshift through the AOM. Note that upshifting or downshifting completely changes the direction of the first-order beam and requires complete realignment of the set up. The various measurements for the two isotopes are listed in Table 2. To check for long term drifts, the measurements were repeated over a period of one month. Each value is an average of ∼40 measurements and has a statistical error of less than 2 kHz. As mentioned in the previous section, to check for optical pumping effects, most measurements were repeated at three values of pump power for a fixed value of probe power.

The most important thing to note from the table is that the measurements at the three powers are consistent with each other. This means that optical-pumping effects are negligible at our level of precision, even when the pump power is increased by a factor of two or more. Note that

Table 2. Hyperfine measurements in ^{85}Rb and ^{87}Rb. The first column gives the transition to which the laser was locked and the second column gives the transition to which the AOM was locked. To check for such optical-pumping errors, the measurements were repeated at three values of pump power, as listed in columns 3–5.

(a) ^{85}Rb

Laser	AOM	Interval (MHz)		
		25 μW	40 μW	70 μW
$2 \to 2$	$2 \to (2,3)$	180.964	180.964	180.978
$2 \to (2,3)$	$2 \to 3$	180.962	180.973	180.970
$3 \to (2,3)$	$3 \to 3$	180.958	180.972	–
$3 \to 3$	$3 \to (2,3)$	180.968	180.964	180.971

(b) ^{87}Rb

Laser	AOM	Interval (MHz)		
		30 μW	40 μW	60 μW
$2 \to 1$	$2 \to (1,2)$	406.115	406.122	406.120
$2 \to (1,2)$	$2 \to 1$	406.119	406.119	406.122
$2 \to (1,2)$	$2 \to 2$	406.114	406.126	406.117
$2 \to 2$	$2 \to (1,2)$	406.120	406.118	406.119

increasing the pump power also increases the height of the peaks in the spectrum, their linewidth, and the overall signal-to-noise ratio. The consistency of the values shows that there are no unknown systematic errors related to these parameters. Finally, the measurements using different transitions are also consistent with one another.

The hyperfine interval in the $5^2P_{1/2}$ state is twice the value listed in Table 2, therefore the average values of the interval are

$$^{85}\text{Rb: } \{F = 3 - F = 2\} = 361.936(14) \text{ MHz},$$
$$^{87}\text{Rb: } \{F = 2 - F = 1\} = 812.238(14) \text{ MHz}.$$

The quoted error is twice the estimated systematic error of 7 kHz in each value obtained by adding the errors in Table 1 in quadrature. To the extent that different transitions have different degrees of systematic error (e.g. due to optical pumping, lineshape distortion, residual magnetic fields, lock-point definition, etc.), the variation in the data will reflect the total error in the measurement. For ^{85}Rb, the 11 values have a standard deviation of 5.8 kHz. For ^{87}Rb, the 12 values have a standard deviation of 3.2 kHz. This suggests that our estimate of 7 kHz is reasonable.

4.1 Hyperfine constants

The average values of the interval can be used to obtain the value of the magnetic-dipole coupling constant A in the $5^2P_{1/2}$ state. The interval is $3A$ for ^{85}Rb, and $2A$ for ^{87}Rb. Thus the hyperfine constants are

$$^{85}\text{Rb: } A = 120.645(5) \text{ MHz},$$
$$^{87}\text{Rb: } A = 406.119(7) \text{ MHz}.$$

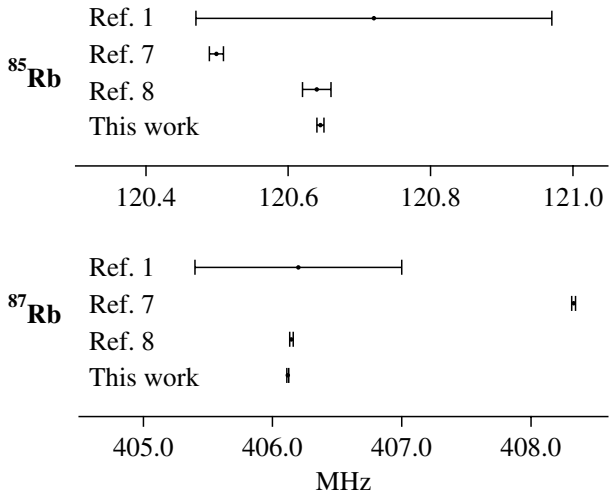

Fig. 3. Hyperfine constants. The figure compares the values of the magnetic-dipole coupling constant A in the $5^2P_{1/2}$ state obtained in this work to earlier values from references [1,7,8].

These values are compared to earlier values in Figure 3. As can be seen, the value for ^{87}Rb from reference [7] is clearly discrepant from both the recommended value [1] and our recent high-accuracy measurement [8]. For ^{85}Rb, the discrepancy is somewhat smaller. Our current values (with the smallest error bars) are completely consistent with our earlier work. In the earlier work, we used a different technique where the absolute frequencies of various hyperfine transitions were measured with a Rb-stabilized ring-cavity resonator. In reference [7], hyperfine intervals were measured by locking frequency-stabilized diode lasers to two transitions and determining their beat frequency with an avalanche photodetector.

5 Conclusion

In summary, we have applied a technique of using an AOM locked to the frequency difference between two hyperfine transitions to measure the hyperfine interval in the $5^2P_{1/2}$ state of Rb. The most important source of systematic error is line shift due to asymmetric pumping into Zeeman sublevels. We check for this error by measuring the same interval for different values of pump power in the saturated-absorption spectrometer. We demonstrate a precision of 7 kHz in the measurement, which resolves large discrepancies between two earlier high-precision measurements of this interval. In future, we plan to apply this technique to measurements in Li and Na, where the hyperfine constants are known with much smaller accuracy.

This work was supported by the Department of Science and Technology, Government of India. One of us (D.D.) acknowledges financial support from the Council of Scientific and Industrial Research, India.

References

1. E. Arimondo, M. Inguscio, P. Violino, Rev. Mod. Phys. **49**, 31 (1977)
2. S.A. Blundell, W.R. Johnson, J. Sapirstein, Phys. Rev. A **43**, 3407 (1991)
3. C.S. Wood et al., Science **275**, 1759 (1997)
4. V.A. Dzuba, V.V. Flambaum, Phys. Rev. A **62**, 052101 (2000)
5. A. Shukla, B.P. Das, J. Andriessen, Phys. Rev. A **50**, 1155 (1994)
6. U.D. Rapol, A. Krishna, V. Natarajan, Eur. Phys. J. D **23**, 185 (2003)
7. G.P. Barwood, P. Gill, W.R.C. Rowley, Appl. Phys. B **53**, 142 (1991)
8. A. Banerjee, D. Das, V. Natarajan, Europhys. Lett. **65**, 172 (2004)
9. Conetic AA Alloy, Magnetic Shield Division, Perfection Mica Co., USA
10. A.J. Wallard, J. Phys. E **5**, 926 (1972)
11. R. Grimm, J. Mlynek, Appl. Phys. B **49**, 179 (1989)
12. G. Hagel et al., Opt. Commun. **160**, 1 (1999)
13. The main effect of laser power in resonance spectroscopy is to broaden the line. It is only at very high powers (compared to the saturation intensity) that the lineshape gets distorted due to the creation of "dressed states". But even under these conditions, the line center remains unaffected